

Sulfur Valence-to-Core X-ray Emission Spectroscopy Study of Lithium Sulfur Batteries

Marko Petric,^{*,†,‡} Ava Rajh,[¶] Alen Vizintin,[§] Sara Drvarič Talian,[§] Robert Dominko,[§] and Matjaž Kavčič^{*,†,¶}

[†]*Jožef Stefan Institute, Jamova 39, 1000 Ljubljana, Slovenia*

[‡]*University of Zagreb, Faculty of Geotechnical Engineering, Hallerova aleja 7, 42000 Varaždin, Croatia*

[¶]*Faculty of Mathematics and Physics, University of Ljubljana, Jadranska ulica 19, SI-1000 Ljubljana, Slovenia*

[§]*National Institute of Chemistry, Hajdrihova 19, 1000 Ljubljana, Slovenia*

E-mail: m.petric@ijs.si; matjaz.kavcic@ijs.si

Abstract

In this work the valence-to-core (VtC) $K\beta$ sulfur X-ray emission spectroscopy (XES) was used to perform quantitative analysis of different sulfur compounds produced in the lithium sulfur (Li-S) battery during discharge. The analysis is based on the theoretical sulfur $K\beta$ XES spectra obtained from the *ab-initio* quantum chemical calculations based on the density functional theory. The emphasis is given on the $K\beta$ sulfur XES spectra of the polysulfide molecules (Li_2S_x , $x = 2, \dots, 8$) produced electrochemically within the Li-S battery. *Ab-initio* molecular dynamics calculations are used further to calculate also the $K\beta$ spectra of Li_2S_x dissolved in a model solvent. Calculated spectra were directly compared with the experimental ones collected with the Johansson type tender XES spectrometer on laboratory synthesized Li_2S_x reference standards and pre-cycled battery cathodes. These results demonstrate that sulfur VtC XES can be used

effectively to analyze quantitatively electrochemical sulfur conversion also in a smaller laboratory without the need for large scale synchrotron facilities.

Due to its high theoretical capacity and energy density, lithium-sulfur (Li-S) batteries are one of the most promising candidates for the next-generation batteries.¹ The fundamental mechanism of Li-S batteries is based on the reduction of sulfur (α -S₈) in the cathode to lithium sulfide (Li₂S) through a series of redox reactions forming intermediate soluble Li₂S_{*x*}, *x* = 2, \dots , 8 polysulfides.² Continuous improvement of the Li-S batteries relies on the level of our understanding of the basic mechanism. Here the development and application of bulk-sensitive nondestructive characterization techniques able to address complex sulfur electrochemical conversion play a major role. Currently, X-ray absorption spectroscopy (XAS) performed at synchrotron beamlines has been most commonly used for this purpose.³⁻⁸ Despite excellent analytical capabilities of XAS, the limited access to synchrotron beamlines represents a bottleneck for more routine analysis. Alternatively, complementary element specific information of sulfur local electronic structure can be obtained using X-ray emission spectroscopy (XES),⁹⁻¹² which can be successfully performed also in a smaller lab employing laboratory excitation sources. However, due to specific tender X-ray range, sulfur XES requires dedicated in-vacuum emission spectrometers being introduced only very recently.¹³⁻¹⁷ Consequently, despite its large potential, sulfur XES has not yet been exploited for the analysis of Li-S batteries.

The terminal sulfur atoms in the Li₂S_{*x*} polysulfides give rise to characteristic pre-edge absorption peak in the measured sulfur XANES spectra¹⁸ and fingerprinting approach using spectra recorded on reference standards is commonly used in XAS analysis on Li-S batteries. Because of less pronounced spectral differences such approach is not applicable in case of XES analysis. Due to disproportionation reactions inevitably leading to the formation of multiple polysulfide species,¹⁹ it is basically impossible to isolate clean pure Li₂S_{*x*} polysulfides, which could be used to obtain reliable XES experimental reference spectrum. In our work, we, therefore, use the analysis based on the theoretical VtC XES spectra of pure polysulfides.

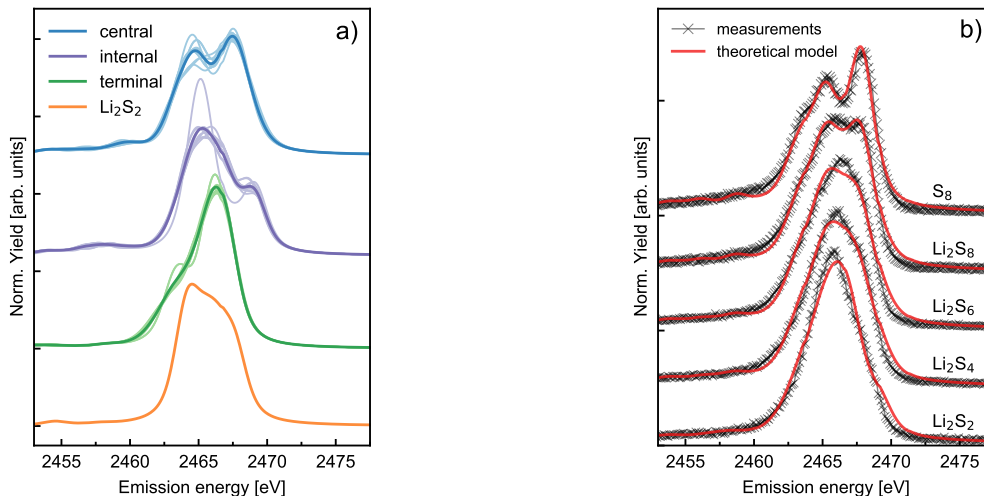


Figure 1: (a) Calculated S VtC XES spectra of the central (blue), internal (violet) and terminal (green) S atoms within the Li_2S_x ($x = 3, \dots, 8$) molecules. Lighter color represents spectra of separate sulfur atoms and darker color represents the average XES spectra of three groups of differently coordinated sulfur atoms within the polysulfide chain. The VtC XES spectrum of the Li_2S_2 molecule differs from XES spectra of terminal sulfur atoms in long chain polysulfides and is plotted separately. (b) Measured high energy resolution proton induced sulfur VtC XES spectra of $\alpha\text{-S}_8$, and Li_2S_x . The fit of the theoretical model to the experimental data is also presented.

These are used to analyze experimental spectra collected from battery cathodes in order to assess the feasibility of the sulfur VtC XES to perform laboratory characterization of Li-S batteries.

The theoretical VtC XES spectra of lithium polysulfides were obtained from first-principles quantum chemical calculations. Two different program packages, StoBe-deMon²⁰ and CP2K/Quickstep,²¹ both based on the density functional theory (DFT)²² approach, were used. Comparison of the sulfur VtC XES of $\alpha\text{-S}$ with both programs is given in Fig. S1, ESI†. After the geometry optimization, VtC XES spectra were calculated for each separate sulfur atom within the Li_2S_x polysulfide molecule. Based on the calculated spectral shape, we can separate three groups of differently coordinated sulfur atoms within a polysulfide molecule. In one group we have terminal sulfur atoms, bound directly to Li atoms on the edge of the polysulfide chain. The second group contents internal atoms inside the chain. In longer polysulfides, with five to eight sulfur atoms, we can additionally separate internal atoms, bonded directly to the

terminal ones, from the atoms in the middle of the chain, which we will refer to as central sulfur atoms from here on. Theoretical average VtC XES spectra for these three groups of differently coordinated sulfur atoms within Li_2S_x polysulfide molecules are presented in Fig. 1a together with XES spectra of each separate sulfur atom within the polysulfide chain. The final theoretical VtC XES spectra of polysulfides were then built as a linear combination of corresponding XES spectra from the terminal, internal and central sulfur atoms (Fig. **S2**, ESI†). The only exception was the Li_2S_2 molecule exhibiting characteristic XES spectrum which differs from the spectra of longer Li_2S_x polysulfides discussed above and was calculated separately. In case of central sulfur atoms in polysulfides and atoms in elemental $\alpha\text{-S}$, the electronic structure of occupied valence orbitals was found very similar and the theoretical VtC XES spectra from these two types of sulfur atoms are practically the same. Besides polysulfides the reduction of S_8 can produce also polysulfide radicals.^{23,24} Especially the radical trisulfur anion S_3^- might play an important role in the electrochemical process.⁴ For that purpose, we have calculated also the VtC spectrum of LiS_3 radical. However, the spectral difference with respect to the spectrum of Li_2S_3 polysulfide (**S4**, ESI†) was found within our experimental uncertainty so radicals were omitted in further discussion.

Table 1: Relative amplitudes of separate spectral contributions obtained from the fitting procedure explained in the text. The error estimates from the fit are given in parentheses.

chemical formula	central atoms	Amplitudes of internal atoms	terminal atoms
S_8	0.98(1)	0.009(6)	0.009(6)
Li_2S_8	0.61(1)	0.195(5)	0.195(5)
Li_2S_6	0.40(1)	0.300(7)	0.300(7)
Li_2S_4	0.32(1)	0.339(6)	0.339(6)
Li_2S_2	0.04(2)	0.43(2)	0.53(1)

In order to validate our theoretical approach, the Li_2S_x polysulfides were synthesized by mixing the stoichiometric amounts of lithium and sulfur in dried tetrahydrofuran. After removing the solvent under reduced pressure, the solid target pellets, suitable for XES measurements, were prepared.²⁵ X-ray emission was induced by irradiating the samples with 2 MeV proton beam and the VtC sulfur spectra were collected with our tender XES spectrom-

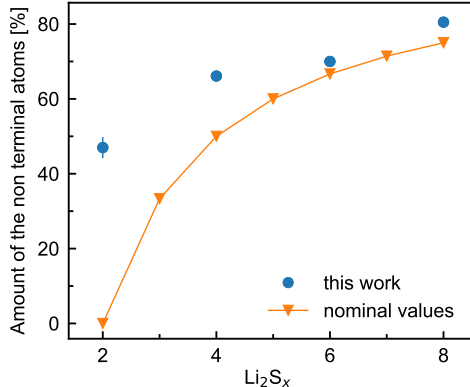


Figure 2: The relative amount of the nonterminal sulfur atoms obtained from the fit compared to the nominal values for pure Li_2S_x polysulfides.

eter.²⁶ The final measured spectra are presented in Fig. 1b. Next, we have built a model spectrum as a linear combination of theoretical VtC XES spectra calculated for the terminal, internal and central sulfur atoms within polysulfide molecules as described previously. This model was fitted to the experimental XES spectra with relative amplitudes of each spectral contribution being the only fitting parameters. In the case of Li_2S_8 , Li_2S_6 and Li_2S_4 , the number of internal and terminal atoms should be the same so relative amplitudes for these two contributions were kept the same during the fit. Results of this fitting procedure are presented in Fig. 1b, where they are compared to the measured spectra, and the relative amplitudes obtained from the fit are given in Table 1. The fitted model describes well the measured spectra, confirming our theoretical model. From the relative amplitudes presented in Table 1, the relative amount of nonterminal (internal+central) sulfur atoms can be obtained, which is a characteristic of the polysulfide chain length. The numbers obtained from the fit can be directly compared to the nominal relative amount of nonterminal atoms expected in pure Li_2S_x polysulfides and this comparison is presented in Fig. 2. Although close agreement is observed for long chain polysulfides, our values start to differ from the nominal ones while going to shorter polysulfides. The difference is most pronounced for the shortest measured polysulfide sample. This is consistent with the results of recent XAS measurements on polysulfide standards where this difference was attributed to the disproportionation re-

actions of lithium polysulfides in solution and precipitation of less soluble short chain solid species.²⁷

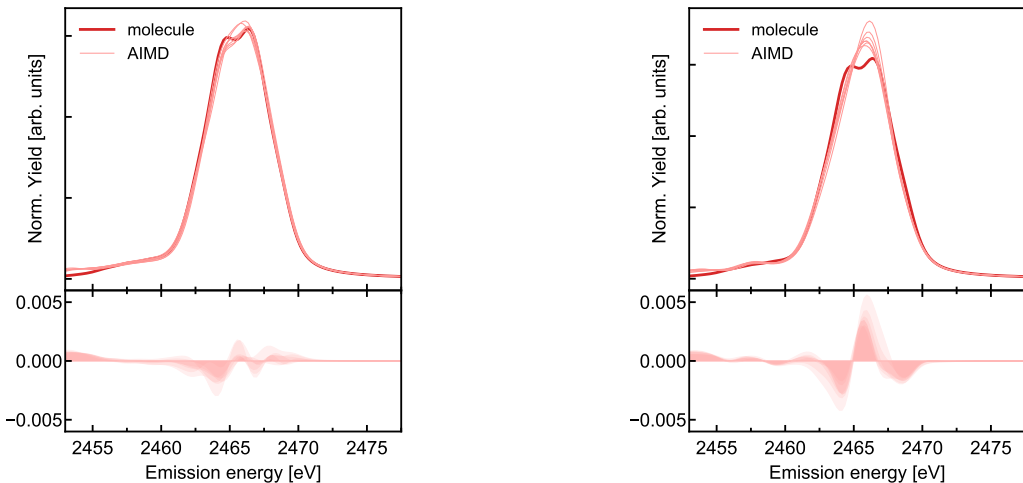


Figure 3: (*top*) Comparison of sulfur VtC XES spectra of isolated Li_2S_7 molecule and (*left*) Li_2S_7 molecule in first (six DOL molecules) and (*right*) second (five DOL and one LiTDI molecule) model solvent. (*bottom*) The relative difference of the XES spectra of Li_2S_7 molecule in both model solvents with respect to the spectrum of isolated Li_2S_7 molecule.

Within a working battery, lithium polysulfides are dissolved in an electrolyte, therefore in the next step we try to study the effect of solvent on the VtC XES spectra. For that purpose, the *ab-initio* molecular dynamics (AIMD) calculations were performed. Since the VtC XES spectra of the terminal, internal and central sulfur atoms calculated for isolated polysulfide molecules were independent of the polysulfide chain length, we can restrict the AIMD calculations to one particular Li_2S_x and the results can be generalized for all polysulfides. The calculations were performed for the Li_2S_7 dissolved in two different model solvents. In the first model Li_2S_7 molecule was surrounded with six 1,3-dioxolane (DOL) molecules and in the second model with five DOL molecules and one 4,5-dicyano-2-(trifluoromethyl)imid-azolid (LiTDI) molecule. We have simulated 21 ps AIMD in the constant volume and temperature ensemble (NVT). The radial distribution functions calculated for Li_2S_7 surrounded with six DOL molecules (Fig. S5, ESI†) were found in good agreement with the work of Kamphaus and Balbuena.²⁸ Sulfur VtC XES spectra were calculated for several consecutive snapshots of the system taken every 3 ps. The final spectra were constructed in the same way as for

isolated polysulfide molecules and normalized to the overall intensity, Fig. 3. Compared to XES spectrum of isolated Li_2S_7 molecule, only minor differences were observed for the first model solvent. In the case of second model, solvent differences are more pronounced, suggesting that the Li-ion in LiTDI might be responsible for this change. This is confirmed by taking an AIMD snapshot at 15 ps and removing from the system all solvent atoms except for lithium. The VtC XES spectra calculated on this modified system exhibit very similar shape as the solvent model, confirming that the Li atom in the solvent is changing the electronic structure of sulfur atoms (Fig. S6, ESI†).

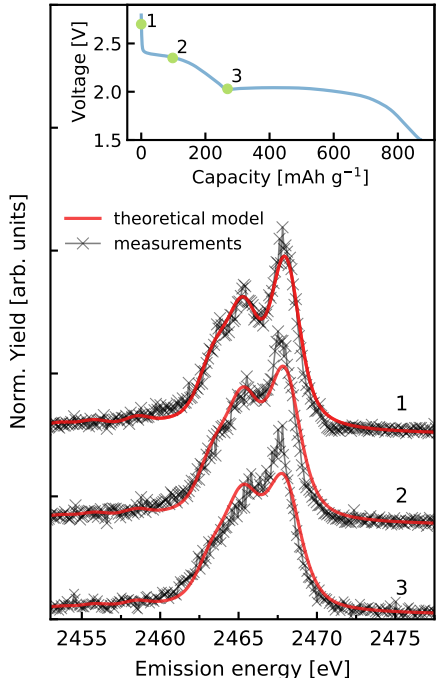


Figure 4: Experimental sulfur VtC XES spectra from several pre-cycled battery cathodes fitted with the theoretical model presented in the text. Electrochemical curve obtained during battery discharge with the points corresponding to our cathode samples is given at the top.

Finally, we tried to use theoretical VtC XES spectra to analyze experimental spectra from Li-S battery cathodes and address electrochemical sulfur conversion during the battery working cycle. For that purpose, MeV proton induced sulfur VtC XES spectra were collected from several pre-cycled battery cathodes which were stopped at different points during the first plateau of the battery discharge curve. Carbon/sulfur composite with PVdF binder and

conductive multiwalled nanotubes was used for battery cathodes and the electrolyte was 1 M LiTDI in TEGDME:DOL.²⁵ The measured spectra of the so-called *ex-situ* samples are presented in Fig. 4 together with the corresponding electrochemical curve obtained during battery discharge. During the first plateau of the discharge curve, the elemental α -S₈ sulfur in the cathode is converted into polysulfides, reaching maximum polysulfide content at the end of the plateau. The formation of Li₂S phases starts at the beginning of the second plateau and it is not discussed in this work. The longer polysulfides (Li₂S₈-Li₂S₅) are expected in our samples and their relative amount should be increasing towards the end of the first plateau. In order to analyze sulfur conversion, two different model spectra were built and fitted to the measured *ex-situ* cathode spectra. The first model was built from the theoretical VtC XES spectra of the terminal, internal and central sulfur atoms in isolated Li₂S_x molecule. The second model was built from XES spectra calculated for Li₂S₇ molecule in a model solvent composed of five DOL and one LiTDI molecule. In this case, calculated XES spectra from the central sulfur atoms within the polysulfide are not anymore the same as for the α -S₈ as it was the case for isolated molecule. In order to take this into account, pure α -S₈ theoretical XES spectrum was additionally included in the model.

Both models were fitted to the experimental cathode spectra with relative amplitudes of separate components being the only free parameters. Similar to the analysis of polysulfide standards, in this case the relative amplitudes of the terminal and internal atoms were also fixed to the same value. The first cathode spectrum corresponds to pure α -S₈, representing the initial cathode state and fitting nicely to the theoretical α -S₈ model spectrum. Both model spectra described above were fitted to the experimental spectra collected from the next two cathodes, and the relative amplitudes of different type of sulfur atoms obtained from both fits are given in Table 2. Within the first model, we cannot resolve XES signal of elemental sulfur from the ones of central sulfur atoms in long chain polysulfides so the relative amplitude for this component actually corresponds to the sum of both contributions. Within the second model, these two signals are resolved and the amplitude of elemental sulfur

given in Table 2 corresponds to the actual amount of initial sulfur remaining in the cathode. Slightly more than half of the initial sulfur has been converted into polysulfides by the end of first plateau, which indicates a bit less efficient conversion compared to the results of previous XAS studies.^{3,5} Most importantly, the general sulfur conversion into polysulfides during battery discharge is clearly confirmed by our results. Also, the relative amplitudes obtained from the fit confirm the formation of predominantly long chain polysulfides. On the other hand, an increase of the relative amount of central sulfur atoms towards the end of the first plateau is observed. This is not consistent with generally expected shortening of the polysulfides along the discharge.

Table 2: Relative amplitudes of different model components obtained from the fit, amplitudes of terminal and internal atoms were kept fixed to the same value during the fit

	Amplitudes of	sample 2	sample 3
model 1	elemental S	0.80(2)	0.69(3)
	internal atoms	0.10(1)	0.16(1)
	terminal atoms	0.10(1)	0.16(1)
model 2	elemental S	0.64(3)	0.48(3)
	central atoms	0.13(6)	0.27(7)
	internal atoms	0.11(3)	0.12(4)
	terminal atoms	0.11(3)	0.12(4)

In this work sulfur VtC XES was used to perform laboratory analysis of sulfur conversion within the Li-S battery cathodes. Sulfur VtC XES spectra of lithium polysulfides in model solvent were obtained from first-principle calculations and used to analyze experimental spectra from polysulfide standards and several pre-cycled Li-S battery cathodes. Our results exhibit high sensitivity of sulfur VtC XES to sulfur electronic structure and demonstrate the feasibility to analyze quantitatively electrochemical sulfur conversion in Li-S battery. XES method is compatible with *operando* measurements on working battery and can also be applied to other upcoming sulfur based systems, such as Mg-S²⁹ and Ca-S.³⁰ Using new dedicated high efficiency tender XES spectrometers¹⁴ and powerful laboratory sources of ionizing radiation, the approach presented here has the potential to bring characterization of sulfur based battery systems from synchrotrons down to smaller laboratories.

This work has been supported by the Slovenian Research Agency programs P1-0112 and P2-0393, research projects N1-0167 and Z2-1863 and by the RADIATE project under the Grant Agreement 824096 from the EU Research and Innovation programme HORIZON 2020.

Conflicts of interest

There are no conflicts to declare.

References

- (1) Wild, M.; O'Neill, L.; Zhang, T.; Purkayastha, R.; Minton, G.; Marinescu, M.; Offer, G. J. Lithium sulfur batteries, a mechanistic review. *Energy Environ. Sci.* **2015**, *8*, 3477–3494, DOI: 10.1039/C5EE01388G.
- (2) Manthiram, A.; Fu, Y.; Chung, S.-H.; Zu, C.; Su, Y.-S. Rechargeable LithiumSulfur Batteries. *Chem. Rev.* **2014**, *114*, 11751–11787.
- (3) Cuisinier, M.; Cabelguen, P.-E.; Evers, S.; He, G.; Kolbeck, M.; Garsuch, A.; Bolin, T.; Balasubramanian, M.; Nazar, L. F. Sulfur Speciation in LiS Batteries Determined by Operando X-ray Absorption Spectroscopy. *J. Phys. Chem. Lett.* **2013**, *4*, 3227–3232.
- (4) Lowe, M. A.; Gao, J.; Abruña, H. D. Mechanistic insights into operational lithiumsulfur batteries by in situ X-ray diffraction and absorption spectroscopy. *RSC Adv.* **2014**, *4*, 18347–18353.
- (5) Dominko, R.; Patel, M. U. M.; Lapornik, V.; Vizintin, A.; Koželj, M.; N. Tušar, N.; Arčon, I.; Stievano, L.; Aquilanti, G. Analytical Detection of Polysulfides in the Presence of Adsorption Additives by Operando X-ray Absorption Spectroscopy. *J. Phys. Chem. C* **2015**, *119*, 19001–19010.

- (6) Wujcik, K. H.; Wang, D. R.; Pascal, T. A.; Prendergast, D.; Balsara, N. P. *J. Electrochem. Soc.* **2016**, *164*, A18–A27.
- (7) Gorlin, Y.; Patel, M. U. M.; Freiberg, A.; He, Q.; Piana, M.; Tromp, M.; Gasteiger, H. A. Understanding the Charging Mechanism of Lithium-Sulfur Batteries Using Spatially Resolved Operando X-Ray Absorption Spectroscopy. *J. Electrochem. Soc.* **2016**, *163*, A930–A939.
- (8) Zhao, E.; Wang, J.; Li, F.; Jiang, Z.; Yang, X.-Q.; Wang, F.; Li, H.; Yu, X. Exploring reaction dynamics in lithium-sulfur batteries by time-resolved operando sulfur K-edge X-ray absorption spectroscopy. *Chem. Commun.* **2019**, *55*, 4993–4996.
- (9) Mori, R. A.; Paris, E.; Giuli, G.; Eeckhout, S. G.; Kavčič, M.; Žitnik, M.; Bučar, K.; Pettersson, L. G. M.; Glatzel, P. Sulfur-Metal Orbital Hybridization in Sulfur-Bearing Compounds Studied by X-ray Emission Spectroscopy. *Inorg. Chem.* **2010**, *49*, 6468–6473.
- (10) Petric, M.; Bohinc, R.; Bučar, K.; Nowak, S. H.; Žitnik, M.; Kavčič, M. Electronic Structure of Third-Row Elements in Different Local Symmetries Studied by Valence-to-Core X-ray Emission Spectroscopy. *Inorg. Chem.* **2016**, *55*, 5328–5336.
- (11) Holden, W. M.; Jahrman, E. P.; Govind, N.; Seidler, G. T. Probing Sulfur Chemical and Electronic Structure with Experimental Observation and Quantitative Theoretical Prediction of K and Valence-to-Core $K\beta$ X-ray Emission Spectroscopy. *J. Phys. Chem. A* **2020**, *124*, 5415–5434.
- (12) Qureshi, M.; Nowak, S. H.; Vogt, L. I.; Cotelesage, J. J. H.; Dolgova, N. V.; Sharifi, S.; Kroll, T.; Nordlund, D.; Alonso-Mori, R.; Weng, T.-C.; Pickering, I. J.; George, G. N.; Sokaras, D. *Phys. Chem. Chem. Phys.* **2021**, DOI: 10.1039/D0CP05323F.
- (13) Malzer, W.; Grötzsch, D.; Gnewkow, R.; Schlesiger, C.; Kowalewski, F.; Van Kuiken, B.;

- DeBeer, S.; Kanngießer, B. A laboratory spectrometer for high throughput X-ray emission spectroscopy in catalysis research. *Rev. Sci. Instrum.* **2018**, *89*, 113111.
- (14) Holden, W. M.; Hoidn, O. R.; Ditter, A. S.; Seidler, G. T.; Kas, J.; Stein, J. L.; Cossairt, B. M.; Kozimor, S. A.; Guo, J.; Ye, Y.; Marcus, M. A.; Fakra, S. A compact dispersive refocusing Rowland circle X-ray emission spectrometer for laboratory, synchrotron, and XFEL applications. *Rev. Sci. Instrum.* **2017**, *88*, 073904.
- (15) Abraham, B.; et al., *J. Synchrotron Radiat.* **2019**, *26*, 629–634.
- (16) Kuzmenko, D.; Vogelsang, U.; Hitz, S.; Müller, D.; Clark, A. H.; Kinschel, D.; Czaplak-Masztafiak, J.; Milne, C.; Szlachetko, J.; Nachtegaal, M. *J. Anal. At. Spectrom.* **2019**, *34*, 2105–2111.
- (17) Rovezzi, M.; et al., *J. Synchrotron Radiat.* **2020**, *27*, 813–826.
- (18) Pascal, T. A.; Wujcik, K. H.; Velasco-Velez, J.; Wu, C.; Teran, A. A.; Kapilashrami, M.; Cabana, J.; Guo, J.; Salmeron, M.; Balsara, N.; Prendergast, D. *J. Phys. Chem. Lett.* **2014**, *5*, 1547–1551.
- (19) Barchasz, C.; Molton, F.; Duboc, C.; Leprêtre, J.-C.; Patoux, S.; Alloin, F. Lithium/Sulfur Cell Discharge Mechanism: An Original Approach for Intermediate Species Identification. *Anal. Chem.* **2012**, *84*, 3973–3980.
- (20) Hermann, K.; et al., StoBe-deMon version 3.1. 2011; <http://www.fhi-berlin.mpg.de/KHsoftware/StoBe/index.html>.
- (21) Kühne, T. D.; et al., CP2K: An electronic structure and molecular dynamics software package - Quickstep: Efficient and accurate electronic structure calculations. *J. Chem. Phys.* **2020**, *152*, 194103.
- (22) Kohn, W. Nobel Lecture: Electronic structure of matter-wave functions and density functionals. *Rev. Mod. Phys.* **1999**, *71*, 1253–1266.

- (23) Wujcik, K. H.; Pascal, T. A.; Pemmaraju, C. D.; Devaux, D.; Stolte, W. C.; Bal-sara, N. P.; Prendergast, D. *Adv. Energy Mater.* **2015**, *5*, 1500285.
- (24) Wang, Q.; Zheng, J.; Walter, E.; Pan, H.; Lv, D.; Zuo, P.; Chen, H.; Deng, Z. D.; Liaw, B. Y.; Yu, X.; Yang, X.; Zhang, J.-G.; Liu, J.; Xiao, J. *J. Electrochem. Soc.* **2015**, *162*, A474–A478, DOI: 10.1149/2.0851503jes.
- (25) Kavčič, M.; Petric, M.; Rajh, A.; Isaković, K.; Vizintin, A.; Talian, S. D.; Dominko, R. Characterization of Li-S Batteries Using Laboratory Sulfur X-ray Emission Spectroscopy. *ACS Appl. Energy Mater.* **2021**, *4*, 2357–2364.
- (26) Kavčič, M.; Budnar, M.; Mühleisen, A.; Gasser, F.; Žitnik, M.; Bučar, K.; Bohinc, R. Design and performance of a versatile curved-crystal spectrometer for high-resolution spectroscopy in the tender x-ray range. *Rev. Sci. Instrum.* **2012**, *83*, 03311.
- (27) Robba, A.; Barchasz, C.; Bučar, K.; Petric, M.; Žitnik, M.; Kvashnina, K.; Vaughan, G. B. M.; Bouchet, R.; Alloin, F.; Kavčič, M. Fingerprinting Mean Composition of Lithium Polysulfide Standard Solutions by Applying High-Energy Resolution Fluorescence Detected X-ray Absorption Spectroscopy. *J. Phys. Chem. Lett.* **2020**, *11*, 5446–5450.
- (28) Kamphaus, E. P.; Balbuena, P. B. First-Principles Investigation of Lithium Polysulfide Structure and Behavior in Solution. *J. Phys. Chem. C* **2017**, *121*, 21105–21117.
- (29) Robba, A.; Vizintin, A.; Bitenc, J.; Mali, G.; Arčon, I.; Kavčič, M.; Žitnik, M.; Bučar, K.; Aquilanti, G.; Martineau-Corcós, C.; Randon-Vitanova, A.; Dominko, R. Mechanistic Study of MagnesiumSulfur Batteries. *Chem. Mater.* **2017**, *29*, 9555–9564.
- (30) Scafuri, A.; Berthelot, R.; Pirnat, K.; Vizintin, A.; Bitenc, J.; Aquilanti, G.; Foix, D.; Dedryvère, R.; Arčon, I.; Dominko, R.; Stievano, L. *Chem. Mater.* **2020**, *32*, 8266–8275.